

UCRL-93008
PREPRINT


CIRCULATION COPY
SUBJECT TO RECALL
IN TWO WEEKS

Artificial Viscosity Q Errors
for Strong Shocks
and More-Accurate
Shock-Following Methods

W. F. Noh

This paper was prepared for submittal to the
Proceedings of the ICFD Conference on Numerical Methods in Fluid Dynamics,
April 1985, Reading University, UK

July 19, 1985



Lawrence
Livermore
National
Laboratory

This is a preprint of a paper intended for publication in a journal or proceedings. Since changes may be made before publication, this preprint is made available with the understanding that it will not be cited or reproduced without the permission of the author.

DISCLAIMER

This document was prepared as an account of work sponsored by an agency of the United States Government. Neither the United States Government nor the University of California nor any of their employees, makes any warranty, express or implied, or assumes any legal liability or responsibility for the accuracy, completeness, or usefulness of any information, apparatus, product, or process disclosed, or represents that its use would not infringe privately owned rights. Reference herein to any specific commercial products, process, or service by trade name, trademark, manufacturer, or otherwise, does not necessarily constitute or imply its endorsement, recommendation, or favoring by the United States Government or the University of California. The views and opinions of authors expressed herein do not necessarily state or reflect those of the United States Government or the University of California, and shall not be used for advertising or product endorsement purposes.

ARTIFICIAL VISCOSITY Q ERRORS FOR STRONG SHOCKS
AND MORE-ACCURATE SHOCK-FOLLOWING METHODS*

William F. Noh

Lawrence Livermore National Laboratory
University of California, Livermore, CA 94550

Abstract

The artificial viscosity (Q) method of von Neumann-Richtmyer¹ is a tremendously useful numerical technique for following shocks wherever and whenever they appear in the flow. We show that it must be used with some caution, however, as serious Q-induced errors ($\approx 100\%$) can occur in some strong shock calculations.

We investigate three types of Q errors:

1. Excess Q heating, of which there are two types: (a) excess Wall Heating on shock formation and (b) Shockless Q Heating;
2. Q errors when shocks are propagated over a non-uniform mesh; and
3. Q errors in propagating shocks in spherical geometry.

As a basis of comparison, we use as our standard the Lagrangian formulation given in Ref. 1 with $Q = C_{00}^2 \ell^2 (u_x)^2$.

This standard Q is compared with Noh's (Q&H) shock-following method,² which employs an artificial heat-flux term (H) in addition to Q, and with the (non-Q) PPM method of Colella and Woodward.³ Both the (Q&H) and PPM methods (particularly when used with an adaptive shock-tracking mesh) give superior results for our test problems.

In spherical geometry, Schulz's tensor Q formulation⁴ of the hydrodynamic equations proves to be most accurate.

*Work performed under the auspices of the U.S. Department of Energy by the Lawrence Livermore National Laboratory under contract No. W-7405-ENG-48.

1. INTRODUCTION

The artificial viscosity (Q) method of von Neumann-Richtmyer¹ has been (and is) a tremendously useful numerical technique for following shocks wherever and whenever they appear in the flow. As we shall see, it must be used with some caution, as serious Q-induced errors can occur in some strong shock calculations.

We investigate three types of Q errors:

- Excess Q heating, of which there are two types: (i) excess Wall Heating on shock formation and (ii) Shockless Q Heating;
- Q errors when shocks are propagated over a non-uniform mesh; and
- Q errors in propagating shocks in spherical geometry.

We use as a basis of comparison, the Lagrangian formulation given in Ref. 1 with $Q = C_0^2 \rho \ell^2 (u_x)^2$, and refer to this as our standard calculation. In Sect. 2, the Lagrangian differential equations with Q [in plane ($\delta = 1$), cylindrical, ($\delta = 2$), and spherical ($\delta = 3$) geometry] are given, and we include an artificial heat flux term $H = h_0^2 \rho \ell^2 |u_x| \epsilon_x$ used in Noh's (Q&H) shock-following method.² For our comparisons, three Q's are defined: Q_L , $Q_L(v)$, and Q_E (where Q_L is our standard Q, above, and $Q_L(v)$ is the original definition given in Ref. 1 (see also Richtmyer-Morton,⁵ p.319) and depends on the geometry $\delta = 1, 2$, or 3). Also two Hs, H_L and H_E , are defined. Here, L refers to the normal Lagrange usage, in which the length ℓ is taken to be equal to the Lagrange mesh interval Δx in the difference formulations, and shocks are spread over a fixed number of mesh intervals (≈ 3) regardless of their actual size. E refers to the Eulerian (or "fixed length") definitions in which ℓ is a constant ($\approx \Delta x_{\max}$), and shocks are spread over a fixed physical distance ($\approx 3\Delta x_{\max}$). Then, in the (Q&H) method, Q_L and H_L are used together, as are Q_E and H_E . Standard (staggered mesh) differencing is used (see Ref. 7), and the nominal benchmark Lagrangian $Q_L = 2\rho(\Delta u)^2$.

In Sect. 3, the Wall Heating Q error is investigated in test problem #1 (Fig. 8). This is an infinite-strength, constant-velocity shock that is generated when a zero-temperature ($\gamma = 5/3$) gas is brought to rest at a rigid wall ($x = 0$). The excess Wall Heating error occurs in the first few zones near the wall (Fig. 1). Now, in nature, heat conduction prevents excess Wall Heating from developing, and thus the (Q&H) method (which includes an artificial heat flux term, H) also prevents the excess Wall Heating error. This is shown in Fig. 2.

The Shockless Q Heating error is investigated using a test problem called "Uniform Collapse."⁶ Here the fluid is shockless, although it is everywhere compressing, and, consequently, an energy error $\Delta\epsilon$ is introduced for Q_L , Q_E , and $Q_L(v)$. In particular, the $Q_L(v)$ error is much larger (for $\delta = 3$) than for Q_L (i.e., it is shown that $\Delta\epsilon_L(v) = \delta^2 \Delta\epsilon_L$), and this fact strongly favors our use of Q_L as the standard Lagrange formulation.

In Sect. 4, the second type of Q error is investigated by introducing a non-uniform mesh ($\Delta x_k = R \Delta x_k$ for constant R) into problem #1 (see Fig. 3). With $Q_L = 2\rho(\Delta u)^2$ as our standard Q, the Q errors for $R = 1.05$ and $R = 1.25$ (Figs. 4 and 5) are compared. The errors are seen to approach 100% for $R = 1.25$, and thus can be a serious concern. A calculation using Q_E (the fixed-length Q), taken together with H_E (in the $(Q_E \& H_E)$ method), eliminates both type #1 and #2 errors (Fig. 6). Unfortunately, using Q_E spreads shocks over a fixed physical distance ($\approx 3\Delta x_{\max}$), which is unacceptable in those regions where a smaller mesh interval occurs. A theoretical explanation for the non-uniform mesh error shows that letting $\ell = \Delta x$ in the difference formulation implies $\ell = \ell(x)$ in the differential equation formulation of Q_L , and it is this use of ℓ that generates this non-uniform mesh error. (For more information see Ref. 7.) The $(Q_L \& H_L)$ method permits the use of a considerably smaller Q_L coefficient, C_0 , and thus produces sharper shocks. This, in turn, produces smaller Q errors, as seen in Fig. 7. The $(Q_L \& H_L)$ method thus offers an acceptable procedure if the unequal zoning is not too severe.

In Sect. 5, the spherical geometry Q errors are investigated using Noh's spherical-shock test problem² (Fig. 8d). This type #3 error is considerably more complicated than the previous Q errors, in that it depends both on the Q formulation [e.g., Q_L vs $Q_L(v)$] and whether or not Q is treated as a scalar viscosity (as in Ref. 1) or as a tensor viscosity, as in Ref. 4. The errors are seen to be truly enormous (Fig. 9), where the error for the standard Q_L formulation is nearly 600% (near the origin) and is nearly 1000% for the original $Q_L(v)$ definition of Q given in Ref. 1. In Fig. 10, we see how serious this error can be as a function of mesh size and just how slow the solution converges to the exact value, $\rho^+ = 64$. Indeed, even for $K = 800$, there is still a considerable error near the origin. The explanation is given in Fig. 11, where it is shown that the error results from the finite shock thickness, and thus the inability of the Q method to select the correct preshock density. That is, the shock spreading picks $\rho^- < \rho_{\text{exact}}^- = 16$. We conclude that sharper shocks give smaller Q errors, and indeed this is shown in Fig. 12, when the (non-Q) PPM method of Woodward and Colella³ produces very

sharp shocks and has minimal error. This error in PPM is further reduced by using an adaptive mesh technique to capture the shocks, and the results using 400 zones (with an adaptive mesh) is equivalent to a normal 1200-zone (essentially converged) PPM problem.

In Sect. 6, Schulz's tensor Q formulation (T) of the hydrodynamic equations is given, along with his tensor $Q_L(S)$ definition.⁴ Calculations using this tensor formulation (Fig. 13) are a significant improvement over the standard scalar (S) solutions (e.g., Fig. 9). However, there is only a slight improvement using Schulz's $Q_L(S)$ over the standard Q_L . Consequently, we conclude that the tensor equations (T) are more important than which Q_L formulation is used. Again, as sharper shocks reduce the type #3 error, nearly exact results are obtained using a very small ($C_0^2 = 1/4$) in the ($Q_L \& H_L$) (T) method, where $Q_L = (1/4)\rho(\Delta u)^2$ and $H_L = 10\rho|\Delta u|\Delta \epsilon$ (Fig. 14). In Fig. 15, the various Q s, ($Q \& H$), and the (non- Q) PPM method are compared. The best results are obtained from the tensor formulation using the ($Q_L \& H_L$) (T) method and PPM with an adaptive mesh.

2. LAGRANGIAN FLUID EQUATIONS WITH ARTIFICIAL VISCOSITY (Q) AND HEAT FLUX (H)

Von Neumann and Richtmyer¹ introduced their artificial viscosity Q as a scalar quantity, and we take their formulation of the Lagrangian fluid equations as our standard. Also, the new ($Q \& H$) shock-following method of Noh² (which uses an artificial heat flux H in addition to the artificial viscosity Q to follow shocks) is included in the formulation.

2.1 Differential Equations

The independent Lagrange variables are r and t , where r is the initial position of the Eulerian (physical) coordinate (i.e., $R(r,0) = r$), and u , ρ , ϵ , and P are the velocity, density, internal energy, and pressure. The differential equations for plane ($\delta = 1$), cylindrical ($\delta = 2$), and spherical ($\delta = 3$) geometries are then (letting $dm = \delta \rho^0 r^{\delta-1} dr = \rho^0 dr^\delta$):

$$\begin{aligned}
 u_t &= -\delta R^{\delta-1}(P+Q)_m & \text{momentum} \\
 R_t &= u \\
 v &= 1/\rho = (R^\delta)_m & \text{mass} \\
 \epsilon_t &= -(P+Q)v_t + \delta(R^{\delta-1}H)_m & \text{energy} \\
 P &= P(\rho, \epsilon) & \text{equation of state}
 \end{aligned} \tag{2.1}$$

2.2 Definitions of Q and H

In Q and H, we include linear terms.^{2,6} These are used in some of the Q error comparisons to produce smoother shock profiles, but otherwise don't affect the Q errors. Also, the Qs and Hs are set to zero if the indicated tests fail to hold.

$$\begin{aligned} \text{Standard Lagrange Q:} \quad Q_L(C_0^2, C_1) &= C_0^2 \rho \ell^2 (u_r)^2 - C_1 \rho C_S \ell u_r, & (2.2) \\ \text{if } u_r < 0; \end{aligned}$$

$$\begin{aligned} \text{Standard Lagrange H:} \quad H_L(h_0^2, h_1) &= h_0^2 \rho \ell^2 |u_r| \epsilon_r + h_1 \rho C_S \ell \epsilon_r, & (2.3) \\ \text{if } Q_L \neq 0; \end{aligned}$$

$$\begin{aligned} \text{Eulerian fixed-length Q:} \quad Q_E(C_0^2, C_1) &= C_0^2 \rho \ell^2 (u_R)^2 - C_1 \rho C_S \ell u_R, & (2.4) \\ \text{if } u_R < 0; \end{aligned}$$

$$\begin{aligned} \text{Eulerian fixed-length H:} \quad H_E(h_0^2, h_1) &= h_0^2 \rho \ell^2 |u_R| \epsilon_R + h_1 \rho C_S \ell \epsilon_R, & (2.5) \\ \text{if } Q_E \neq 0; \end{aligned}$$

$$\begin{aligned} \text{Original Lagrange formulation}^1: \quad Q_L(v) &= (C_0^2 \rho \ell^2)^2 \rho \left(\frac{r}{R}\right)^{2\delta-2} (v_t)^2, & (2.6) \\ \text{if } v_t < 0; \end{aligned}$$

where C_0 , C_1 , h_0 , and h_1 are constants, ℓ is a constant with the dimensions of length, and C_S is the local sound speed. The usage is $(Q_L \& H_L)$ and $(Q_E \& H_E)$. Equation (2.6) is the original Q formulation (see also Ref. 5, p. 319) in terms of $v = (1/\rho)$, and we note it is the only Q here to depend on the geometry (δ). In the Lagrange formulation (L), the standard use is to take $\ell = \Delta r$ in the difference equations. This spreads shocks over a fixed number (≈ 3) of mesh intervals (regardless of their size), while in the Eulerian formulation (E), ℓ is constant ($\approx \Delta x_{\max}$), and shocks are spread over a fixed physical length ($\approx 3\ell$). Standard "staggered mesh" difference equations are used (see Ref. 7 for details), and the nominal Q_L benchmark difference formulation is $Q_L = 2\rho(\Delta u)^2$.

3. EXCESS Q HEATING

There are two excess Q heating errors: (1) excess wall (or piston) heating due to Q, which occurs on shock formation (e.g., at a rigid wall where a gas is brought to rest, and a shock is propagated away, or for the sudden startup of a piston); and (2) Q heating for shockless compressions (e.g., when $u_r < 0$, but no shock is present).

3.1 The Wall Heating Error Test Problem

Test problem #1 is that of a constant-state, constant-velocity shock of infinite strength (i.e., the pre-shock pressure $p^- = p^0 = 0$). The shock is generated in a perfect ($\gamma = 5/3$) gas by bringing the cold ($\epsilon^0 = 0$) gas to rest at a rigid wall at $x = 0$. This is just the familiar constant-velocity (piston) shock, but in a frame of reference where the piston (here a rigid wall) is at rest (Fig. 8a,b). In Fig. 1, ρ^+ is plotted for our "standard calculation" using $Q_L = 2\rho(\Delta u)^2$. The shaded area (the Wall Heating error) occurs typically in the first three zones next to the wall (or piston). That this error is unavoidable for any shock smearing method, is argued in Ref. 7.

In real fluids, heat conduction is present, and Wall Heating does not occur, and this is the basis of Noh's (Q&H) method, Eqs. (2.1) and (2.3). In Fig. 2, $Q_L(0.67, 0.2)$ is used, plus the heat flux term $H_L(0, 3/4) = 3/4\rho C_S \Delta \epsilon$. As expected, the Wall Heating error is zero. We also note that the $(Q_L \& H_L)$ solution is considerably smoother, and this permits the use of much smaller Q constants C_0 and C_1 (with generally smaller Q errors).

3.2 Shockless Q Heating Errors

This is the situation where a compression wave exists (i.e., $u_r < 0$), and thus $Q \neq 0$; yet the exact solution is shockless. For this analysis, we consider the useful "Uniform Collapse Problem" (see Noh,⁶ p. 60), in which a flow is everywhere undergoing a compression, but no shock develops. We consider a unit "sphere" ($0 \leq r \leq 1$), (for $\delta = 1, 2$, or 3), and to simplify the analysis of the energy errors due to Q , we assume pressure to be a function of density only, $P = P(\rho)$.

The initial values are $u(r, 0) = -r$, $\rho = \rho^0$, $\epsilon = \epsilon^0$, and $P^0 = P(\rho^0)$, with boundary conditions $u(0, t) = 0$ and $u(1, t) = -1$. The exact solution is that the fluid simply coasts with its initial velocity (i.e., $u = -r$) until all points uniformly collapse onto the origin $R = 0$, at time $t = 1$. It is easy to verify that the exact solution is given by

$$u(r, t) = -r, \quad R = r(1-t), \quad \text{and} \quad v = (1/\rho) = (1-t)^\delta (1/\rho^0). \quad (3.1)$$

Thus, $\rho = \rho(t)$, $P = P(\rho) = P(t)$, and since $\epsilon_t = -Pv_t = \delta/\rho^0 P(t) (1-t)^{\delta-1}$, then $\epsilon = \epsilon(t)$.

It follows that $Q = Q(t)$, and thus the solution given by Eq. (3.1) continues to hold, except for the energy equation. If we let the error in energy be $\Delta \epsilon = \int (\epsilon_t + Pv_t) dt = - \int Qv_t dt$, then from Eq. (3.1) and $\tau = (1-t)$,

$$\Delta \epsilon_L = -\int Q_L v_t dt = -\delta (C_0 \ell)^2 \ln(\tau) , \quad (3.2)$$

$$\Delta \epsilon_E = -\int Q_E v_t dt = \frac{1}{2} \delta (C_0 \ell)^2 \tau^{-2} , \text{ and} \quad (3.3)$$

$$\Delta \epsilon_L(v) = -\int Q_L(v) v_t dt = -\delta^3 (C_0 \ell)^2 \ln(\tau) . \quad (3.4)$$

We note that

$$\Delta \epsilon_L(v) = \delta^2 \Delta \epsilon_L , \text{ and } \Delta \epsilon_L < \Delta \epsilon_E . \quad (3.5)$$

Now, as $\tau \rightarrow 0$, the error $\Delta \epsilon \rightarrow \infty$, and this Shockless Q Heating error can indeed be serious. From Eq. (3.5) and ($\delta = 3$), we see that the error $\Delta \epsilon_L(v)$ is nearly an order of magnitude greater than the error $\Delta \epsilon_L$. It is due to arguments similar to these that Noh in 1956⁶ suggested that the Q_L of Eq. (2.2) be taken as the standard Q formulation for all geometries $\delta = 1, 2$ or 3 . We make the suggestion again (and for more reinforcement, see Figs. 9 and 10), since $Q_L(v)$ still seems to be in common use.

4. Q ERRORS FOR A NON-UNIFORM MESH

The second type of Q error occurs when shocks are propagated over a mesh with unequal intervals. In problem #1, let

$$\Delta x_{k+1} = R \Delta x_k , \quad (4.1)$$

where R is a constant: $1 \leq R \leq 2$. We investigate the cases $R = 1.05$ and $R = 1.25$. In order to show the errors for both decreasing ($R < 1$) and increasing ($R > 1$) mesh intervals, we let the mesh decrease for the first half of the problem, then increase for the second half (Fig. 4). In Fig. 5, $R = 1.05$, and the density is plotted for our standard $Q_L = 2\rho(\Delta u)^2$. The total error is shaded, and again we see the familiar Wall Heating error in the first several zones. The new error, $\Delta \rho_L^+ = \rho_L^+ - \rho_{\text{exact}}^+ = \rho_L^+ - 4$, is > 0 for the first half (decreasing mesh), and $\Delta \rho_L^+ < 0$ for the second half. This new (type #2) non-uniform mesh error grows with R and becomes very serious ($\approx 100\%$) for $R = 1.25$. This is unfortunate, since it is not uncommon to use $R = 2$ in practice, and thus $R = 1.25$ might well be considered a modest zoning change.

The good news is shown in Fig. 6, where $R = 1.05$, and the Eulerian "fixed length" Q_E is seen to eliminate the non-uniform mesh error. When Q_E is used

in conjunction with H_E in the $(Q_E \& H_E)$ method, then both the type #1 (Wall Heating) error and the type #2 (non-uniform mesh) error are completely eliminated. The bad news is that very large Q_E constants are necessary [where $(C_0 \ell)^2 = (C_0 \Delta x_{\max})^2 = 6$ (for $C_0 = 1$) and $C_1 \Delta x_{\max} = 0.8$ (for $C_0 = 0.33$)], and this is seen to spread the shock over a large number of the smaller zones. In this regard, the use of Q_E is not satisfactory.

A more practical solution is to use the $(Q_L \& H_L)$ method. This eliminates the Wall Heating error, and (as mentioned earlier) the use of the heat flux term H permits the use of a much smaller Q_L constant C_0 (and C_1), which, in turn, reduces the type #2 (non-uniform) mesh error. In Fig. 7, $R = 1.05$ and $Q_L = \rho(\Delta u)^2$ (i.e., $C_0^2 = 1$) is compared with the $(Q_L \& H_L)$ method, with a corresponding reduction in the non-uniform zoning error to around 3%.

4.1 Theoretical Discussion

In the standard Lagrange difference formulation of Q_L , the length ℓ in Eq. (2.2) is taken to be $\ell = \Delta x$, and thus $(\ell u_x) = (\Delta u)$. Now, when an unequal mesh interval is used, Δx is no longer a constant, and this implies that $\ell = \ell(x)$ in the differential formulation of Q_L in Eq. (2.2). In fact, where Δx_k is given by Eq. (4.1), $\ell(x)$ is found to be

$$\ell(x) = 2[(R-1)x + \Delta x_0]/(R+1) . \quad (4.2)$$

See Ref. 7 for details and further explanation of the non-uniform mesh error.

One consequence of using Eq. (4.2) in Eq. (2.2) in the differential equations, Eq. (2.1), is that steady traveling shocks are no longer solutions. This is clear since the shock width (instead of being a constant) will now be proportional to $\ell(x)$. This would still be an acceptable numerical approximation for shocks if only the proper shock jump conditions held, but our numerical experiments show that this is unfortunately not the case.

5. Q ERRORS IN SPHERICAL ($\delta = 3$) GEOMETRY

The third type of Q error is related to strong shock propagation in spherical (or cylindrical) geometries. This error is considerably more serious (up to 1000% error in (excess) shock heating near the origin), and is also more complicated than the previous Q errors. This third type of Q error depends on the Q formulation [i.e., Q_L of Eq. (2.2) vs. $Q_L(v)$ of Eq. (2.6)] and also

seems to depend on whether Q is treated as a scalar or a tensor viscosity in the formulation of the hydrodynamic equations. In particular, a tensor formulation (Sect. 6) due to Schulz⁴ gives sharper shocks than our standard use of Q_L in Eq. (2.1), and this is instrumental in reducing this third type of Q error.

Test problem #3 is just the spherical ($\delta = 3$) generalization of test problem #1 where the post (infinite) shock solutions (u^+ , ρ^+ , ϵ^+ , and P^+) are, again, constant step-value functions (Fig. 8d).

Our standard test problem has 100 mesh intervals ($\Delta r = 0.01$), and the results are compared at time $t = 0.6$. Since the shock speed is $S = 1/3$, then 80% of the mesh (i.e., 80 mesh points) have been traversed by the shock, and one would expect accurate results. Unfortunately, this is not the case, as is seen in Fig. 9, where the standard $Q_L(2) = 2\rho(\Delta u)^2$ is compared with the original $Q_L(v) = 2(\Delta r)^2 \rho \left(\frac{r}{R}\right)^4 \left(\frac{\Delta v}{\Delta t}\right)^2 = 2\rho \left[\Delta u + \frac{2u\Delta R}{R}\right]^2$. Here, both are compared with the exact solution, $\rho^+ = 64$. The numerical results are strikingly poor and, in fact, hardly bear any resemblance to the exact solution. The error for the standard $Q_L = 2\rho(\Delta u)^2$ is on the order of 600% near the origin and 20% behind the shock, while the error for the original von Neumann-Richtmyer Q [here $Q_L(v)$ of Eq. (2.6)] is roughly 1000% in the central region and nearly 40% behind the shock. Clearly this third type of Q error depends on the Q formulation. The solution using $Q_L(v)$ is seen to be definitely inferior to the solution using Q_L . There are several reasons for this. One is related to the Shockless Q Heating Error of Sect. 3. Here, the first zone of test problem #3 is just a special case of the Uniform Collapse test problem, and we found in Eq. (3.5) that the Q_L energy errors went as $\Delta \epsilon_L < \Delta \epsilon_L(v) = \delta^2 \Delta \epsilon_L$. Thus, for $\delta = 3$, the error using $Q_L(v)$ is 9 times as large as using Q_L . There is an even mahead of ore disquieting error in using $Q_L(v)$, in that it preheats the gas the shock. This occurs because, in the preshocked region (Fig. 9d), $v = 1/\rho = (1 + \frac{t}{R})^{-2}$, and thus $v_t \leq 0$, and $Q_L(v) \neq 0$. This preheating is, of course, not physical (and is another instance of a shockless Q Heating error - note that Q_L does vanish as it should), and this error combines with the large Shockless Q Heating error near the origin to produce the poor results of curve (2) in Fig. 9. It's amazing that the shock solution is as good as it is. Just how slowly the $Q_L(v)$ solution converges is shown in the comparisons of Fig. 10, where the results are plotted for various mesh intervals: $K = 50$ ($\Delta r = 0.02$); $K = 100$ ($\Delta r = 0.01$), up to $K = 800$, where $\Delta r = 0.00125$. Even at $K = 800$, the numerical solution still has an unacceptable error. These results show that $Q_L(v)$ of Eq. (2.6) is a poor formulation and is essentially

the reason that our definition of Q_L given by Eq. (2.2) is taken to be the standard Q (for $\delta = 1, 2$, and 3). We stress this point since $Q_L(v)$ still seems to be in common use.

Now, of course, these are still serious errors in the use of the standard $Q_L = 2\rho(\Delta u)^2$. This difficulty is analyzed in Fig. 11. The problem is associated with the shock smearing due to Q . Because of the finite shock thickness, the calculation "senses" an incorrect (too small) jump-off value of the preshocked density (ρ^-). That is, the shock smearing selects a $\rho^- < \rho_{\text{exact}}^- = 16$. This error is a maximum at early times and becomes less serious as time advances as the (similarity) solution spreads out the preshocked region over more and more mesh points. Thus, a given shock thickness produces less and less error as time increases. The key, then, to more accuracy is to sharpen shocks as much as possible.

The non- Q PPM method of Woodward and Colella³ produces very sharp shocks (on the order of one-to-two mesh widths), and their results are considerably more accurate than the use of the standard Q_L . This is shown in Fig. 12. Also, the PPM results on the standard $K = 100$ problem are compared with their very accurate "adaptive mesh shock-following procedure" using $K = 400$. The $K = 400$ results are also shown to be nearly as accurate (converged) as the standard PPM with $K = 1200$. The effect of using an adaptive mesh is to minimize the actual (i.e., physical) shock thickness, and, as we've argued in Fig. 11, is all-important in determining the correct preshocked value $\rho^- = 16$. Clearly, using an adaptive mesh for resolving shocks is an important procedure, and such a method would be equally effective for any Q [or (Q&H)] shock-following procedure.

6. SCALAR VS TENSOR Q FORMULATIONS

In 1964, Schulz⁴ proposed that Q be treated as a tensor viscosity and gave the following (T) formulation of the hydrodynamic equations (for $\delta = 1, 2$, and 3). We include the von Neumann-Richtmyer scalar (S) formulation, Eq. (2.1), again for comparison. Also, the use of the artificial heat flux (H) remains the same:

$$\begin{aligned} \rho u_t + P_R &= -Q_R \\ \rho(\epsilon_t + P v_t) &= -Q[u_R + (\delta-1)\frac{u}{R}] - \frac{1}{R^{\delta-1}} [R^{\delta-1} H]_R \end{aligned} \quad \text{Scalar (S)} \quad (6.1)$$

$$\begin{aligned} \rho u_t + P_R &= -[Q_R + (\delta-1)\frac{Q}{R}] \\ \rho(\epsilon_t + P v_t) &= -Q u_R - \frac{1}{R^{\delta-1}} [R^{\delta-1} H]_R \end{aligned} \quad \text{Tensor (T)} \quad (6.2)$$

Schulz also defined a new Q , which we denote by

$$Q_L(S) = C_0^2 \ell^2 |u_{rr}|^{3/2} |u_r|^{1/2}, \quad (6.3)$$

if $u_r < 0$, and 0 otherwise, and as usual, $\ell = \Delta r$ in the difference formulation.

Now, Schulz's $Q_L(S)$ doesn't produce the Shockless Q Heating error of Sect. 3 (since $u_{rr} = 0$, and thus $Q_L(S) = 0$ for the Uniform Collapse Problem), and we thus might expect superior results for our spherical test problem #3. Indeed, the results (Fig. 13) using the tensor formulation, Eq. (6.2), with $Q_L(S)$ and Q_L are significantly better than using the scalar (S) equations, Eq. (6.1), but there is essentially no improvement using $Q_L(S)$ over Q_L . We conclude, then, that the major improvement occurs because shocks are narrower (for any Q) in the tensor (T) formulation. The reasons why shocks are sharper is not entirely clear, but it follows, in part, from the formulation Eq. (6.2), where we note that there is less Qdv shock heating than for the scalar equations, Eq. (6.1). That is, $Qdv \rightarrow Qu_R$ independently of geometry ($\delta = 1, 2$, or 3) in Eq. (6.2). The $(Q_L \& H_L)(T)$ method [i.e., Eq. (6.2)] with a small Q constant $C_0^2 = 1/4$ is particularly accurate. This is shown in Fig. 14, where we compare $Q_L(1/4)(T)$ (which indeed has a narrower shock, but is extremely noisy) with $[Q_L(1/4) \& H_L(10)](T)$. These $(Q_L \& H_L)(T)$ results are reasonably smooth behind the shock and are essentially exact. Thus, we find the best all-around results for the 100-zone test problem are given by the $(Q_L \& H_L)(T)$ shock-following method using Schulz's tensor formulations, Eq. (6.2), or by using the (non- Q) PPM method with an adaptive shock-following mesh.

The results are summarized in Fig. 15, where we compare the various Q_L s, $(Q_L \& H_L)$, and the PPM method.

REFERENCES

1. J. Von Neumann and R.D. Richtmyer, "A Method for the Numerical Calculation of Hydrodynamical Shocks," J. Appl. Phys. 21, 232 (1950).
2. W.F. Noh, Artificial Viscosity (Q) and Artificial Heat Flux (H) Errors for Spherically Divergent Shocks, Lawrence Livermore National Laboratory, Livermore, CA, UCRL-89623 (1983).
3. P. Colella and P. Woodward, The Piecewise-Parabolic Method (PPM), Lawrence Berkeley Laboratory, Berkeley, CA, LBL-14661 (1982).
4. W.D. Schulz, "Tensor Artificial Viscosity for Numerical Hydrodynamics," J. Math. Phys. 5, 133 (1964).
5. R.D. Richtmyer and K.W. Morton, "Difference Methods for Initial-Value Problems," Second Edition, Interscience Tracts in Pure and Applied Mathematics (Interscience, NY, 1967).
6. W.F. Noh, Numerical Methods in Hydrodynamic Calculations, Lawrence Livermore National Laboratory, Livermore, CA, UCRL-52112 (1976).
7. W.F. Noh, Artificial Viscosity Errors for Strong Shocks, Lawrence Livermore National Laboratory, Livermore, CA, UCRL-53669 (1985).

FIGURE CAPTIONS

FIG. 1. $Q_L = 2\rho(\Delta u)^2$. Shaded area is "Wall Heating Error."
Typically it is over three mesh intervals.

FIG. 2. The (Q&H) method, where $Q_L(2/3,1/5) = 2/3\rho(\Delta u)^2 + 1/5 \rho C_s |\Delta u|$ and $H_L(0,3/4) = 3/4\rho C_s \Delta \epsilon$. The heat flux term, H, reduces the Wall Heating error to zero.

FIG. 3. The unequal-zoned, infinite-shock test problem. Initial and boundary conditions are the same as test problem #1 (see Fig. 8b). Here, the mesh interval decreases for the first half of the mesh ($R < 1$), then increases for the second half ($R > 1$).

FIG. 4. Standard $Q_L(2,0) = 2\rho(\Delta u)^2$, and $R = 1.25$. The type #2 error ($\Delta \rho = \rho - 4$) is positive for the first half, where the mesh interval decreases ($R < 1$), and $\Delta \rho > 0$ for the second half ($R > 1$). The type #1 Wall Heating error is present in the first few zones next to the rigid wall on the left.

FIG. 5. Standard $Q_L(2,0) = 2\rho(\Delta u)^2$, and $R = 1.25$. Here the error is very serious ($\approx 100\%$).

FIG. 6. $R = 1.05$, and we compare the fixed-length Q_E with the $(Q_E \& H_E)$ method.

(1) $Q_E(6,0.8) = 6\rho(\frac{\Delta u}{\Delta X})^2 - 0.8\rho C_s(\frac{\Delta u}{\Delta X})$ this eliminates the non-uniform mesh error.

(2) $Q_E(6,0.8) \& H_E(0,6) = 6\rho C_s(\frac{\Delta \epsilon}{\Delta X})$, which eliminates both the type #1 Wall Heating error and the non-uniform mesh type #2 error. However, there is too much shock spreading over the finely zoned regions using Q_E for this to be a practical way to minimize these errors.

(3) Exact solution.

FIG. 7. $R = 1.05$, and we compare Q_L (with reduced coefficient $C_0 = 1$) with the $(Q_L \& H_L)$ method.

(1) $Q_L(1,0) = \rho(\Delta u)^2$. The solution is noisy, but type #1 and #2 errors are reduced.

(2) $Q_L(1,0) = \rho(\Delta u)^2$ & $H_L(0,2/3) = 2/3\rho C_s \Delta \epsilon$. Using both Q_L and H_L (with small Q coefficients) eliminates the Wall Heating type #1 error altogether and reduces the non-uniform mesh type #2 error to $\approx 3\%$. The $(Q_L \& H_L)$ method is much smoother than Q_L alone and may be a practical compromise for mesh-interval changes that aren't too large.

FIG. 8. The exact solution at $t = 0.6$ to Noh's Generic Constant-Velocity Shock problems²: (a) initial conditions; (b) plane geometry ($\delta = 1$) with a shock generated at a rigid wall; (c) a shock generated at the axis of symmetry for a cylinder ($\delta = 2$); and (d) a shock generated at the center of a sphere ($\delta = 3$). All solutions have constant post-shock states, and all have the same constant shock speed, $S = 1/3$ (for initial conditions (a) and $\gamma = 5/3$). The essential difference is the preshocked density: $\rho^- = 1$ for $\delta = 1$; $\rho^- = 4$ for $\delta = 2$; $\rho^- = 16$ for $\delta = 3$; where $\rho = \rho^0(1 + t/R)^{\delta-1}$ in front of the shock.

FIG. 9. (1) Standard $Q_L = 2\rho(\Delta u)^2$.
 (2) $Q_L(v) = 2(\Delta r)^2 \rho(\frac{r}{R})^4 (\frac{\Delta v}{\Delta t})^2$ [the original von Neumann-Richtmyer Q formulation, Eq. (2.6)]. Here, Q_L is superior to $Q_L(v)$, but both Q s are in serious error. The correct solution is $\rho^+ = 64$.

FIG. 10. This example shows the truly large errors (in density) using the original $Q_L(v) = 2(\Delta r)^2 (r/R)^4 (\Delta v/\Delta t)^2$ for various mesh intervals (Δr). The comparisons are $t = 0.6$ and $\Delta r = 0.01, 0.01, 0.005$, and 0.00125 , or $K = 50, 100, 200$, and 800 . This shows that the convergence of the density to the correct value $\rho^+ = 64$ is very slow indeed, and even for $K = 800$, the error is unacceptable.

FIG. 11. The solution for Noh's spherical test problem (Fig. 8d) is given at two different times ($t = 6$ and $t = 30$) for the scale variable, $\xi = t/R$. As t increases, the preshock density profile is spread over a physically greater and greater distance. Hence, the preshock value $\rho^- = 16$ should be progressively easier to resolve numerically as time advances. The wiggly line is the numerical solution using the standard $Q_L = 2\rho(\Delta u)^2$. The numerical error is so large ($20\% \leq \epsilon \leq 600\%$) that it hardly resembles the exact solution, $\rho^+ = 64$.

FIG. 12. The (non-Q) PPM method of Woodward and Colella³ has very narrow shocks (1 or 2 mesh intervals), and, for the standard test problem, ($K = 100$) gives superior results. PPM using mesh refinement (i.e., a shock-capturing adaptive mesh with $K = 400$) is equivalent to the standard PPM using $K = 1200$. It is clear that using an adaptive mesh is a very important procedure for accurately tracking shocks.

FIG. 13. The lower curve uses our standard $Q_L(2,0) = 2\rho(\Delta u)^2$, but is cast in Schulz's tensor formulation, Eq. (6.2). The upper curve also uses Schulz's tensor formulation, Eq. (6.2), along with his $Q_L(S) = \rho|\Delta u|^2$ of Eq. (6.3). We see that the results are essentially the same for either Q_L formulation. We conclude, then, that it is the tensor use of Q that is important, rather than the particular choice of Q_L . Consequently, we stay with the standard $Q_L = 2\rho(\Delta u)^2$ usage.

FIG. 14. A comparison of $Q_L(T)$ and the $(Q_L \& H_L)(T)$ method [i.e., Eq. (6.2)] using a very small Q_L constant $C^2 = 1/4$. Here, the $Q_L(1/4) = 0.25\rho(\Delta u)^2(T)$ formulation is very noisy, but produces a narrow shock. The sharp shock remains in the $[Q_L(1/4) \& H_L(10)](T)$ method [where $H_L(10) = 10\rho|\Delta u|\Delta\epsilon$], and we see that most of the post-shock noise is damped, and the density and energy errors are nearly zero. Thus, the $(Q_L \& H_L)(T)$ method is a preferred shock-following procedure.

FIG. 15. We compare all of the methods for the standard $K = 100$ test problem and for both the scalar (S) and tensor (T) formulations [Eqs. (6.1) and (6.2)]. The (non-Q) PPM Method lies between the scalar $Q_L(S)$ and $(Q_L \& H_L)(S)$ results, but is not as accurate as the $Q_L(T)$ and the $(Q_L \& H_L)(T)$ results. PPM with mesh refinement, curve (5), and the $(Q_L \& H_L)(T)$ method, curve (6), give essentially the converged (exact) solution and are the preferred methods.

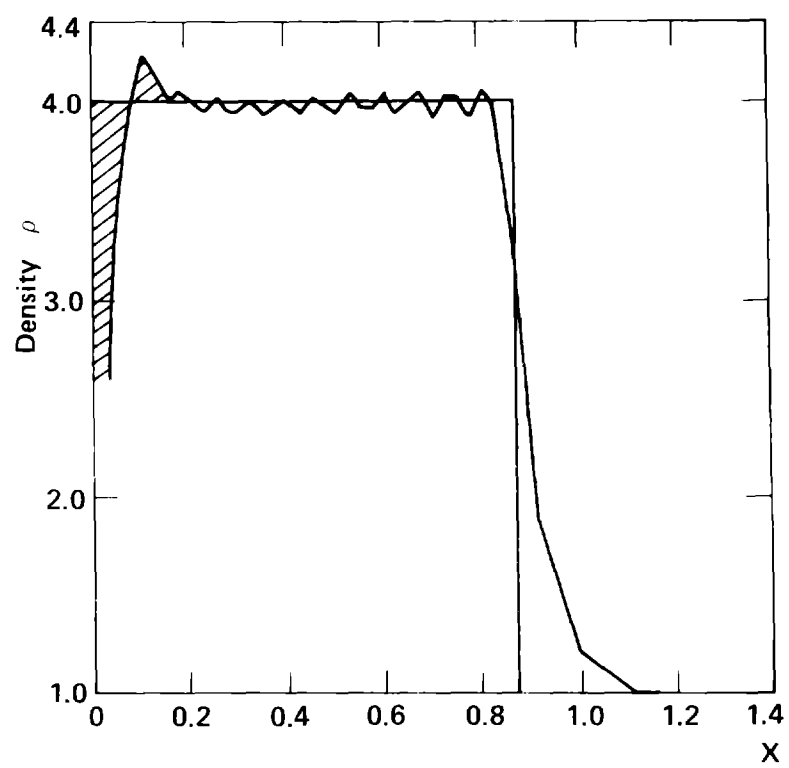


Fig. 1

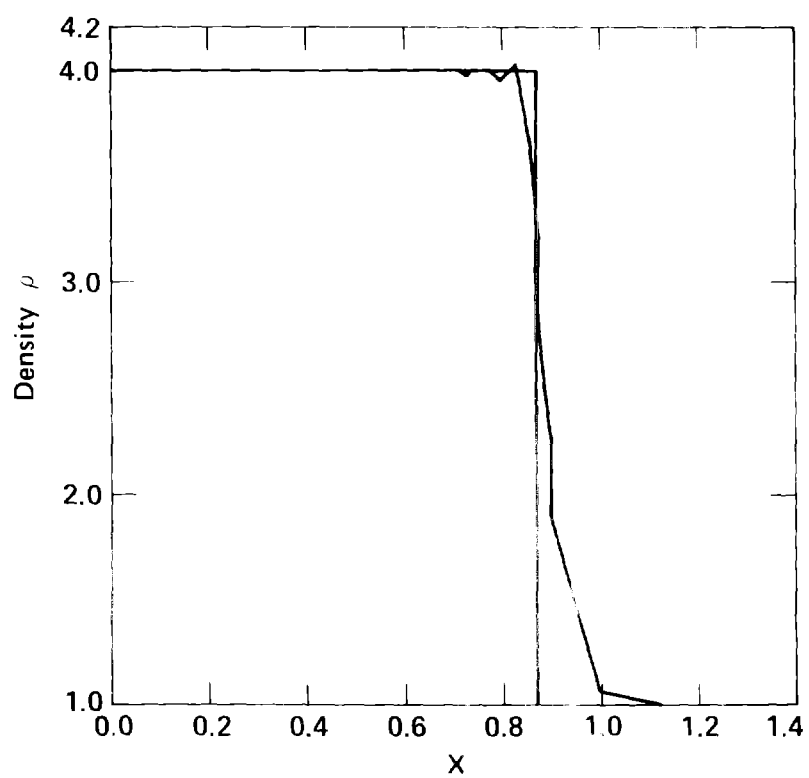


Fig. 2

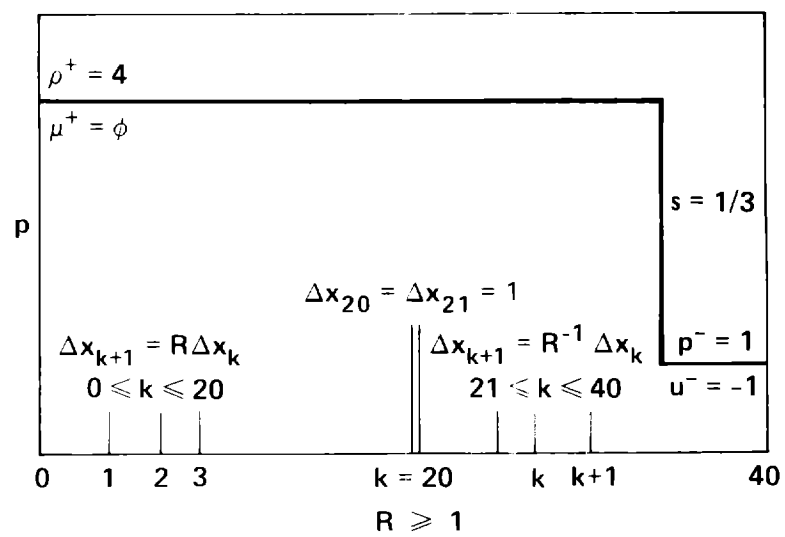


Fig. 3

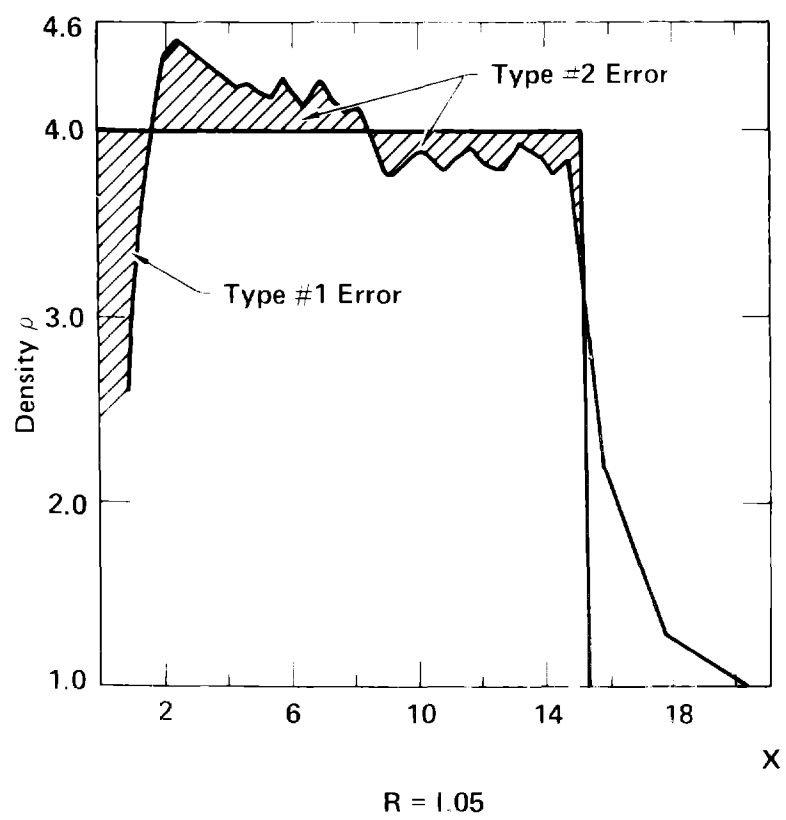


Fig. 4

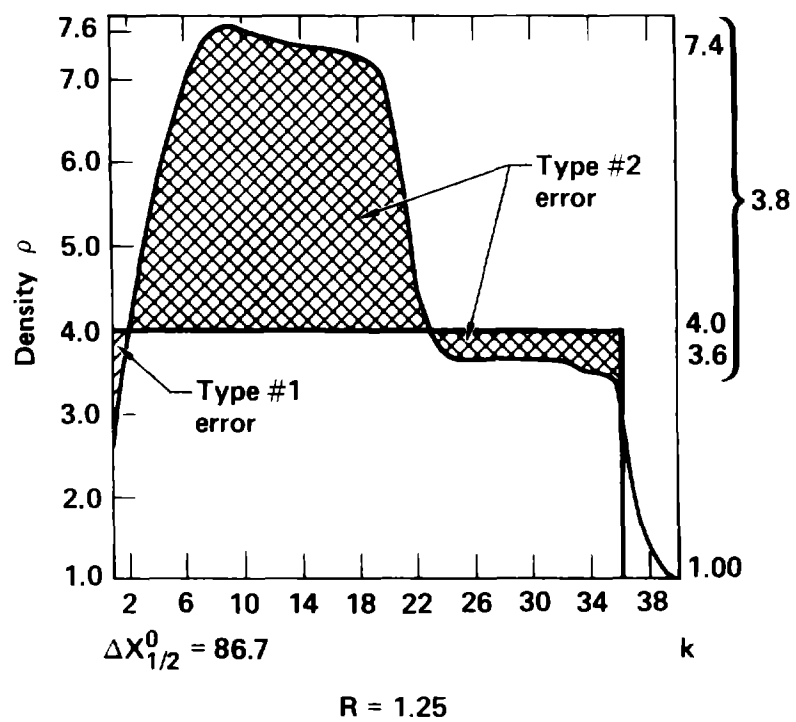


Fig. 5

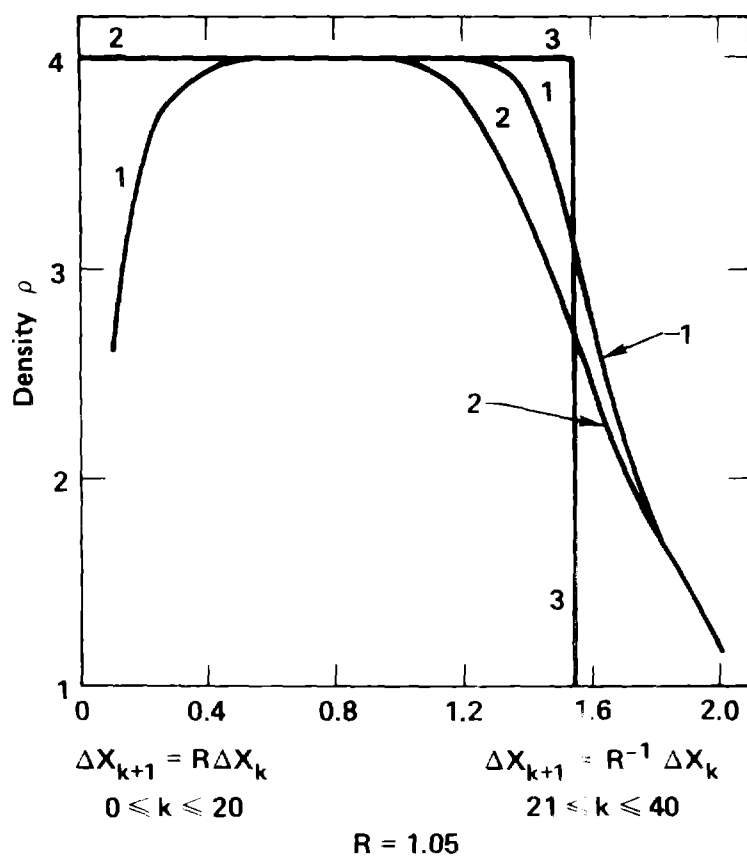


Fig. 6

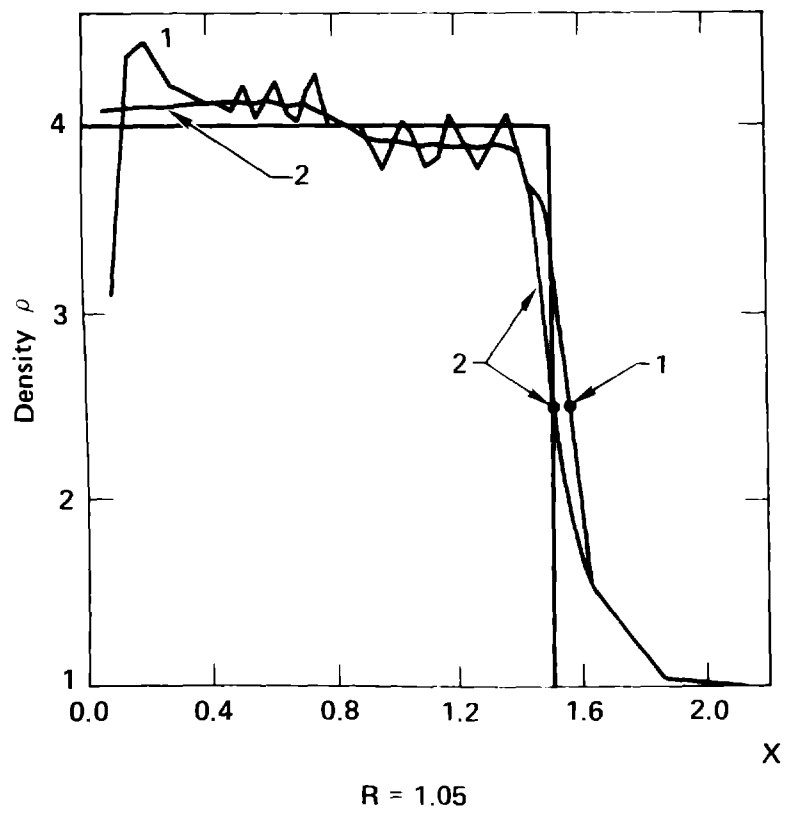


Fig. 7

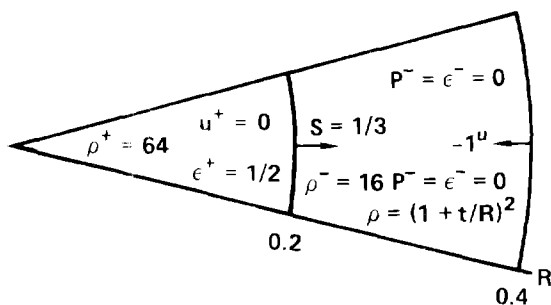
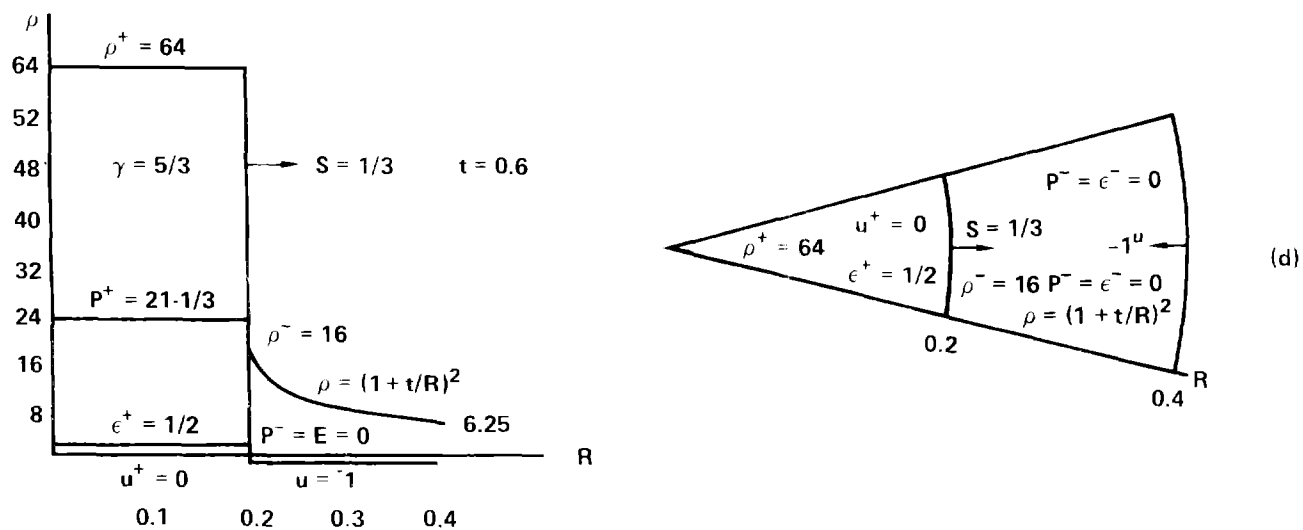
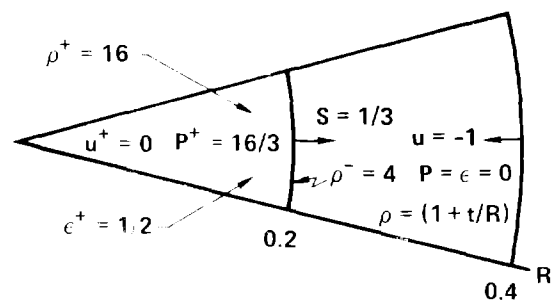
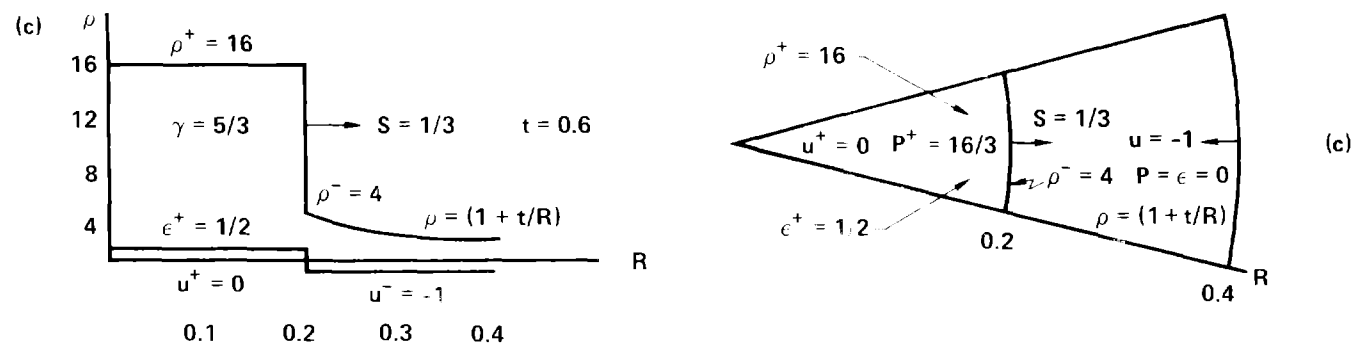
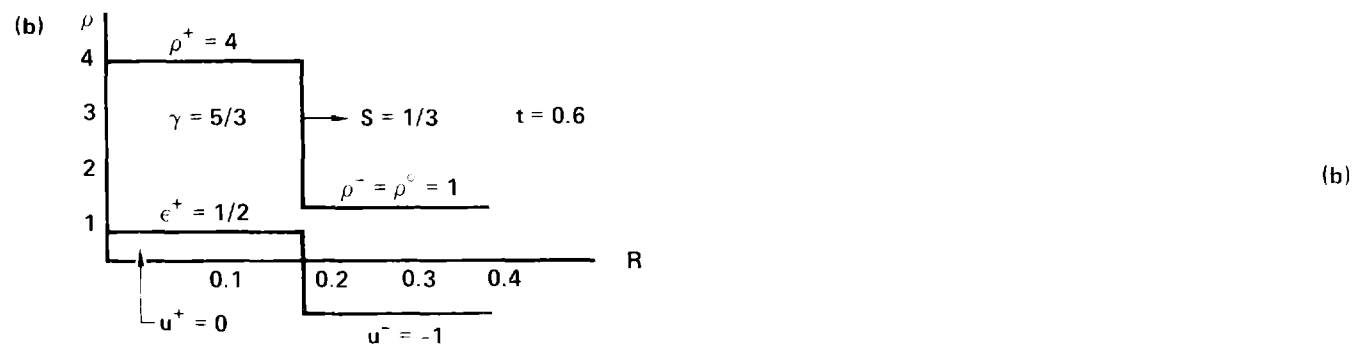
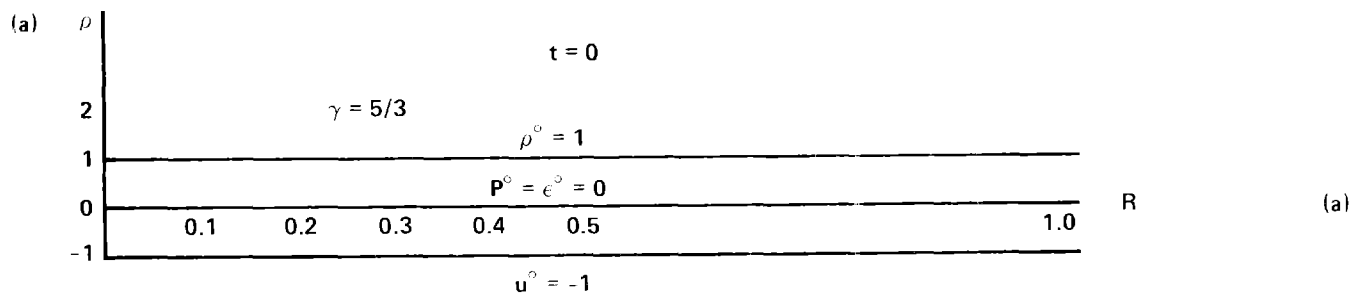


Fig. 8

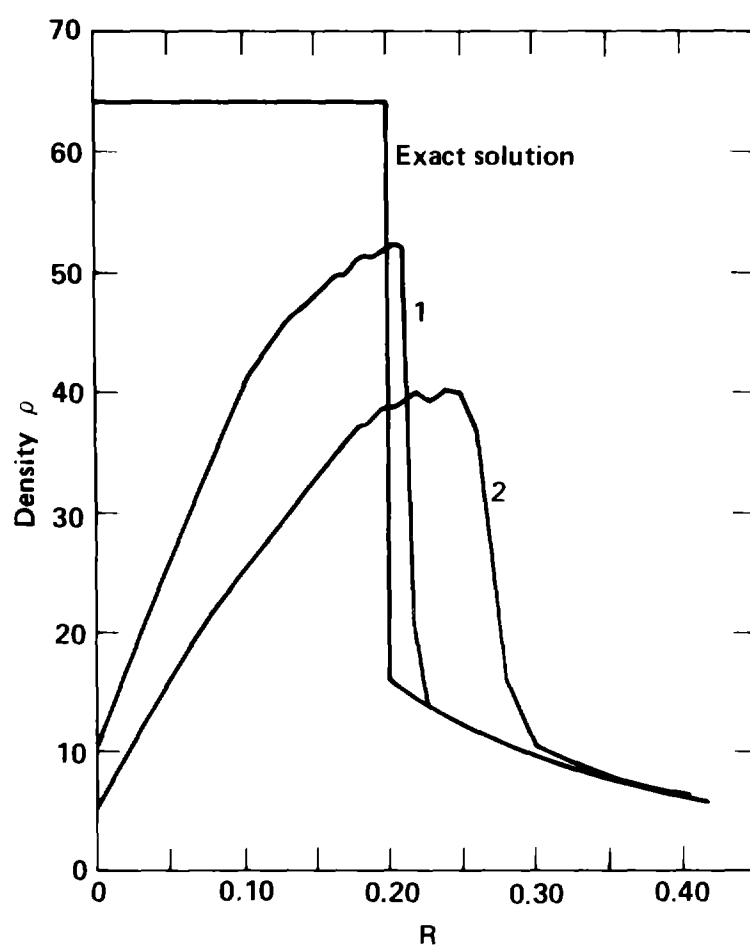


Fig. 9

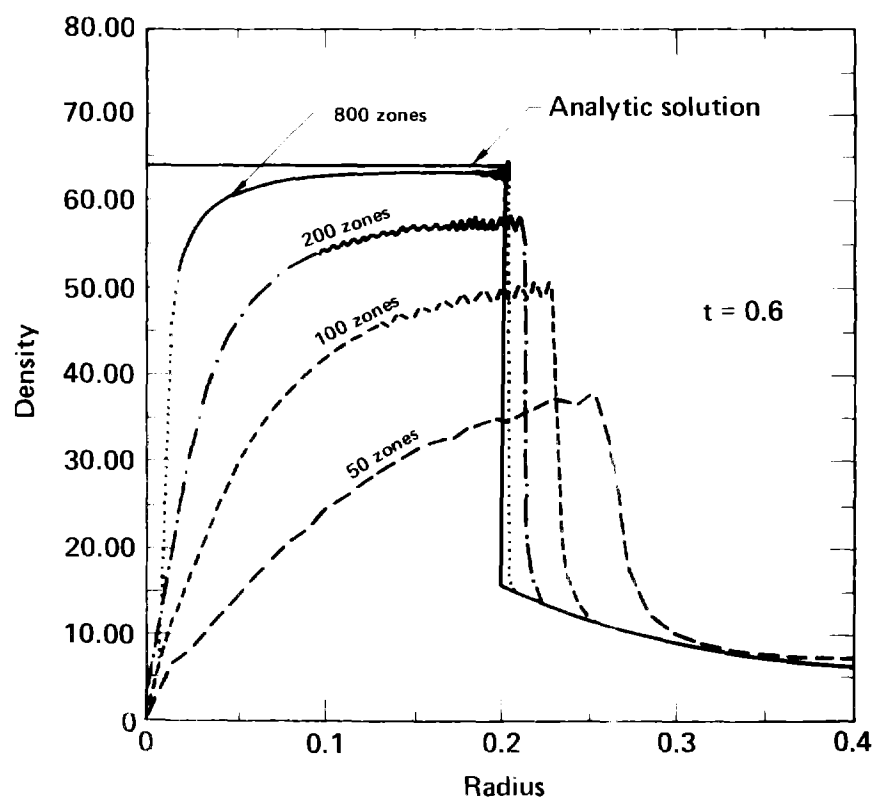


Fig. 10

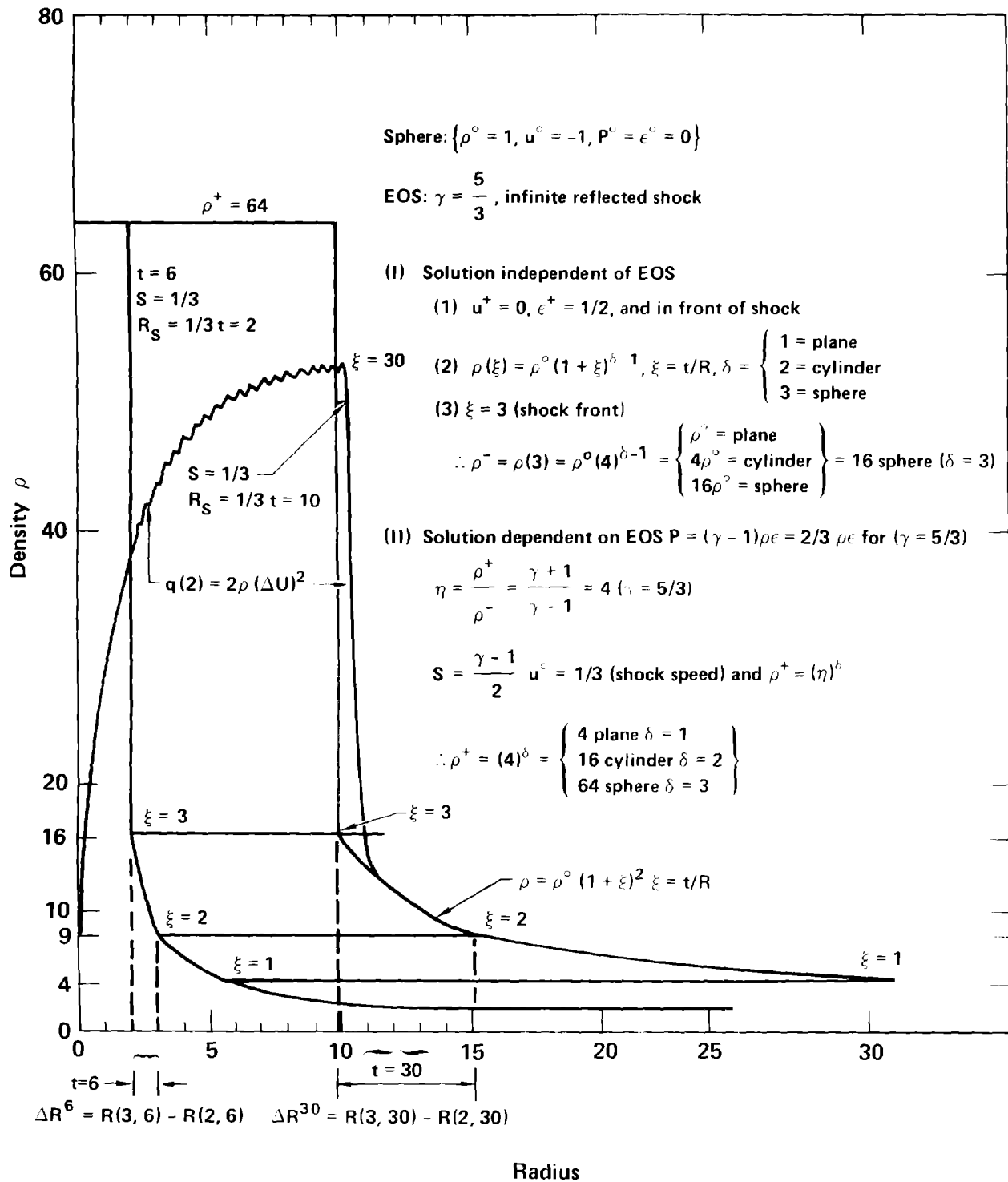


Fig. 11

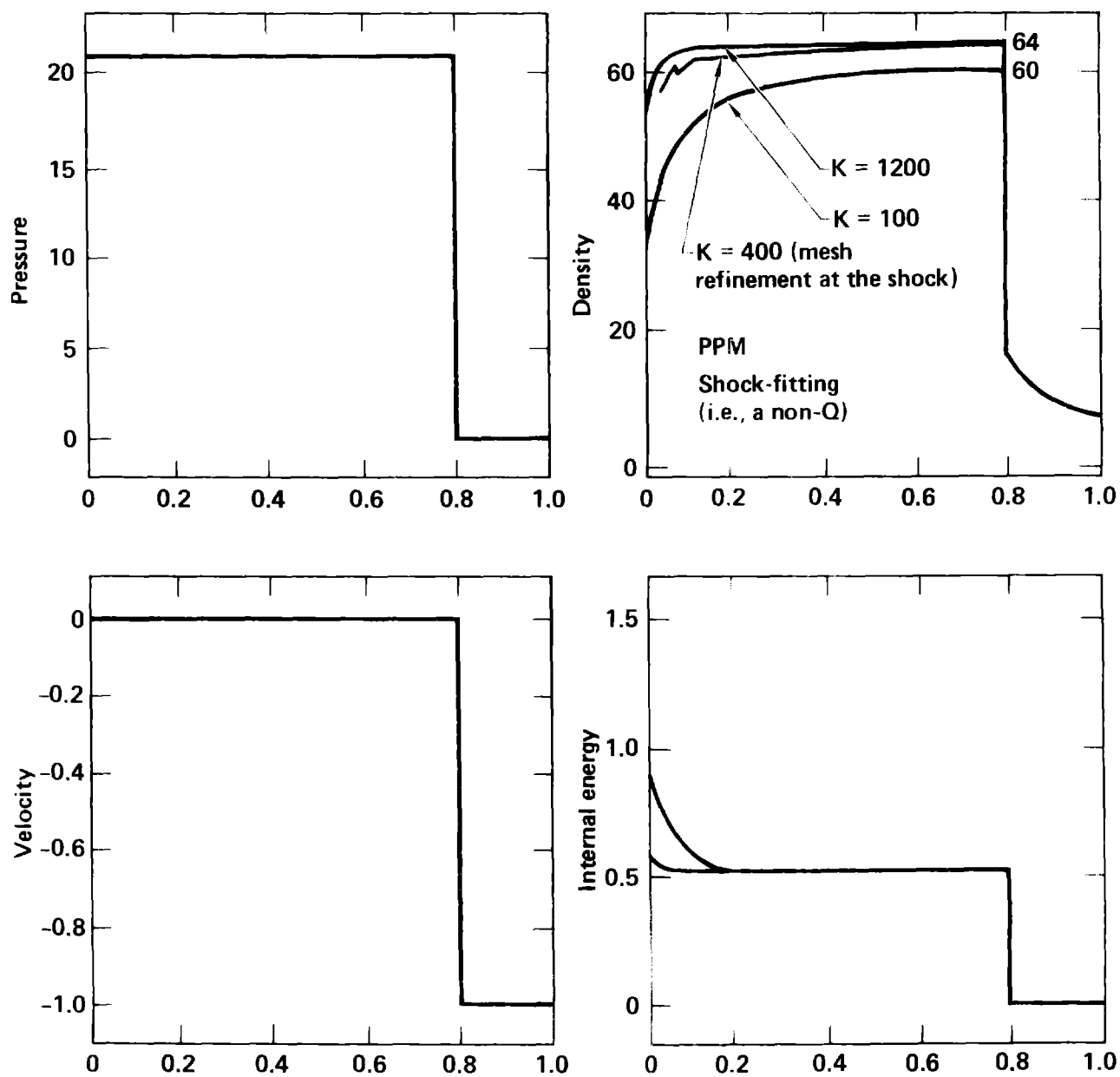


Fig. 12

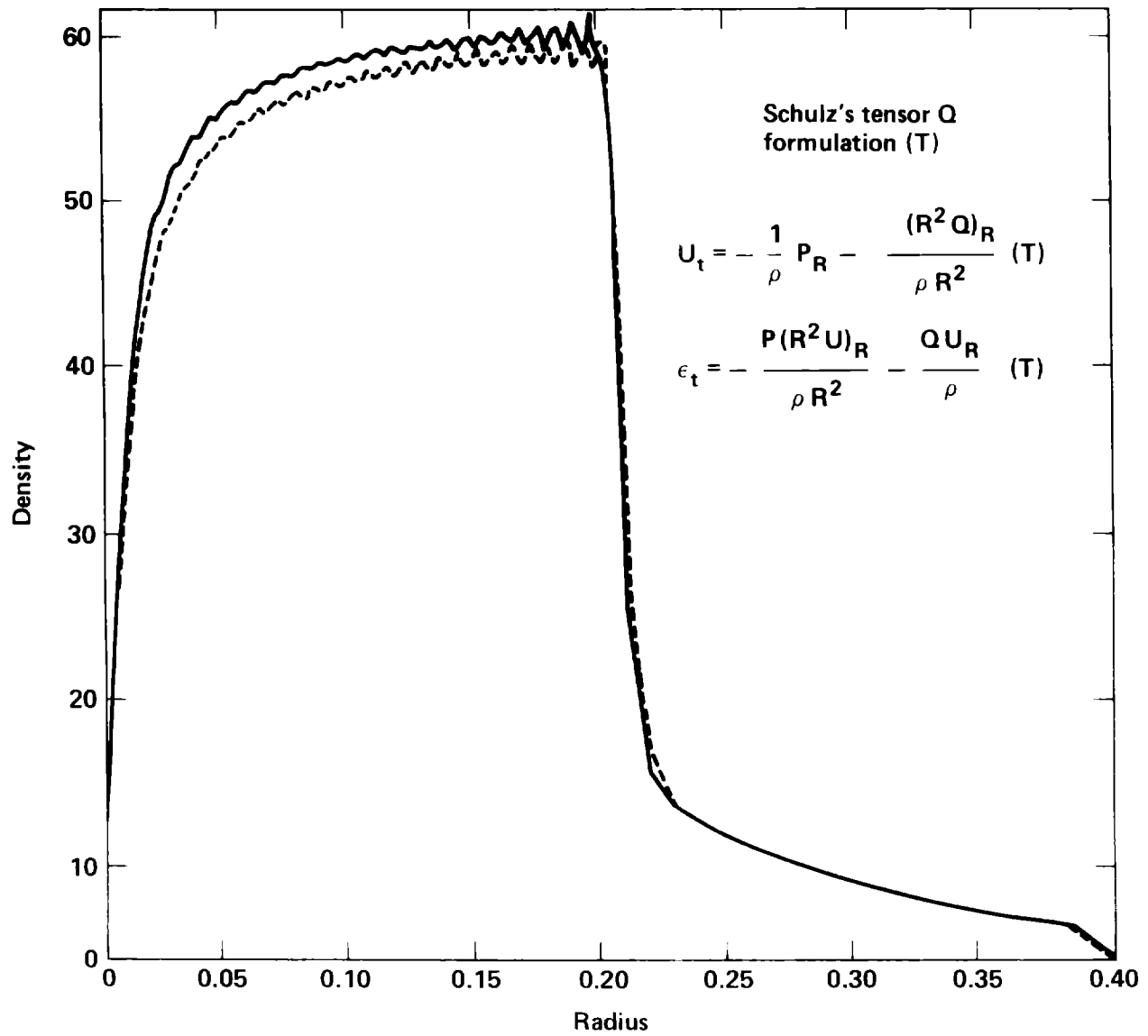


Fig. 13

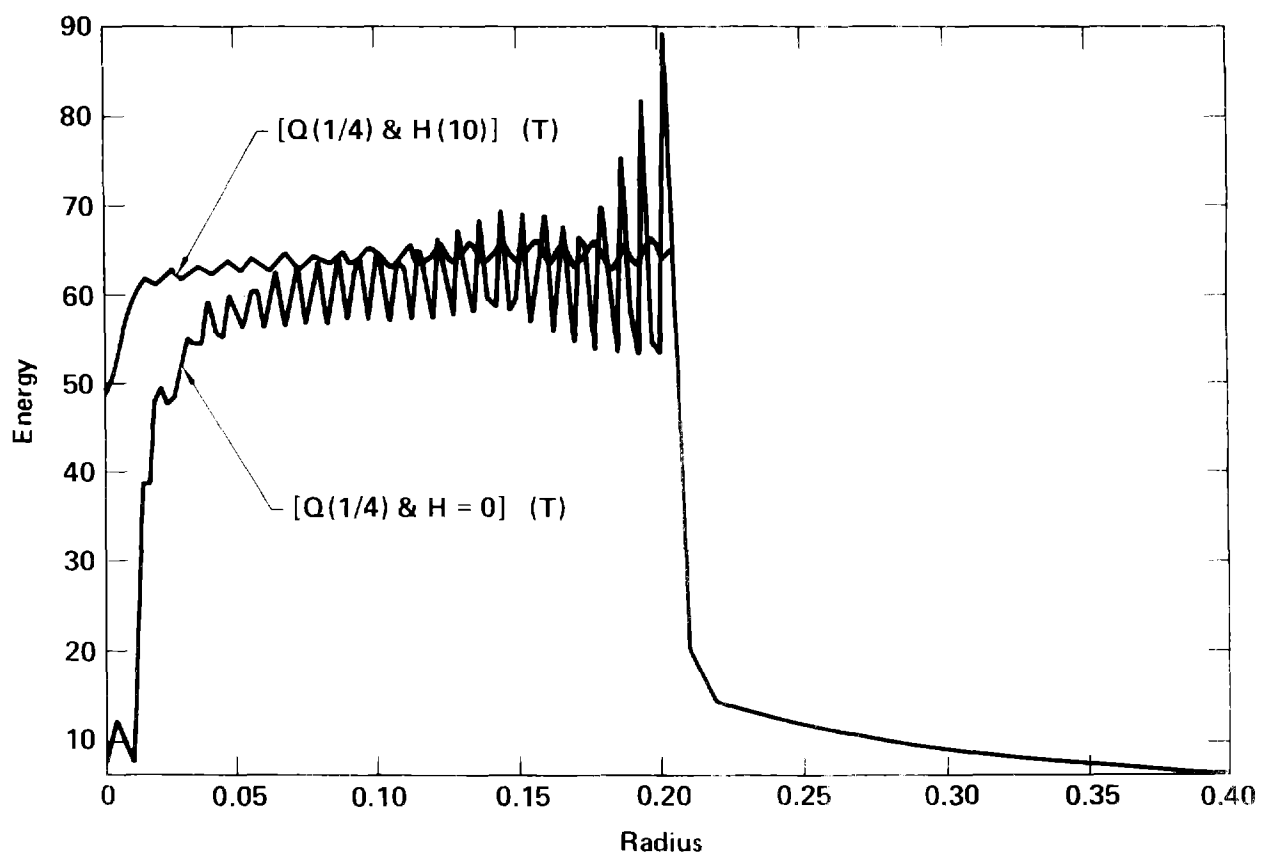


Fig. 14

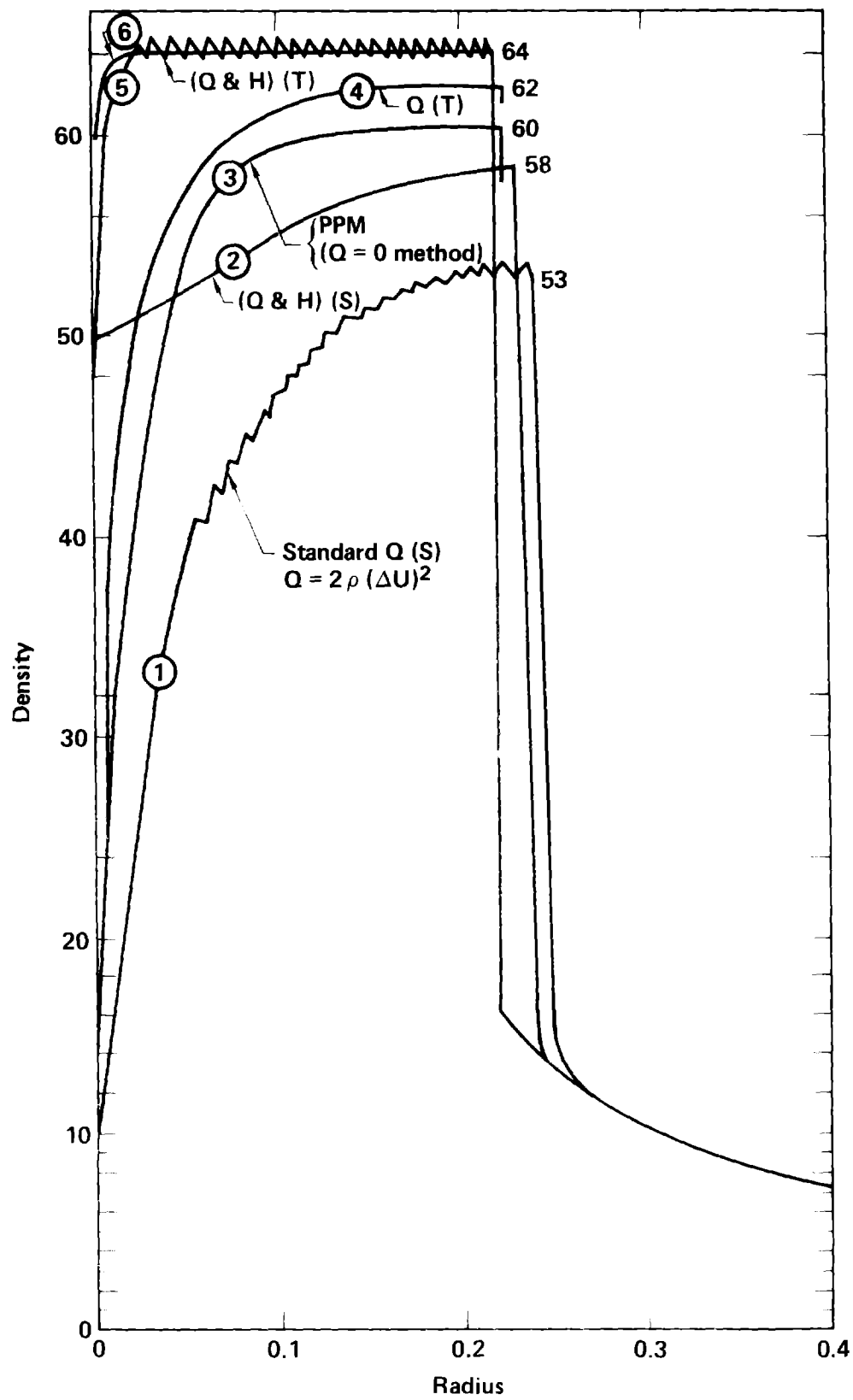


Fig. 15